JVI Journals.ASM.org

SLAM- and Nectin-4-Independent Noncytolytic Spread of Canine Distemper Virus in Astrocytes

Lisa Alves,[a,b,c] Mojtaba Khosravi,[a,c] Mislay Avila,[a,c] Nadine Ader-Ebert,[a,c] Fanny Bringolf,[a,c] Andreas Zurbriggen,[a] Marc Vandevelde,[a,b] Philippe Plattet[a]

Division of Neurological Sciences, Department of Clinical Research and Veterinary Public Health, Vetsuisse Faculty, University of Bern, Bern, Switzerland[a]; Division of Neurological Sciences, Department of Clinical Veterinary Medicine, Vetsuisse Faculty, University of Bern, Switzerland[b]; Graduate School for Cellular and Biomedical Sciences, University of Bern, Bern, Switzerland[c]

ABSTRACT

Measles and canine distemper viruses (MeV and CDV, respectively) first replicate in lymphatic and epithelial tissues by using SLAM and nectin-4 as entry receptors, respectively. The viruses may also invade the brain to establish persistent infections, triggering fatal complications, such as subacute sclerosis pan-encephalitis (SSPE) in MeV infection or chronic, multiple sclerosis-like, multifocal demyelinating lesions in the case of CDV infection. In both diseases, persistence is mediated by viral nucleocapsids that do not require packaging into particles for infectivity but are directly transmitted from cell to cell (neurons in SSPE or astrocytes in distemper encephalitis), presumably by relying on restricted microfusion events. Indeed, although morphological evidence of fusion remained undetectable, viral fusion machineries and, thus, a putative cellular receptor, were shown to contribute to persistent infections. Here, we first showed that nectin-4-dependent cell-cell fusion in Vero cells, triggered by a demyelinating CDV strain, remained extremely limited, thereby supporting a potential role of nectin-4 in mediating persistent infections in astrocytes. However, nectin-4 could not be detected in either primary cultured astrocytes or the white matter of tissue sections. In addition, a bioengineered "nectin-4-blind" recombinant CDV retained full cell-to-cell transmission efficacy in primary astrocytes. Combined with our previous report demonstrating the absence of SLAM expression in astrocytes, these findings are suggestive for the existence of a hitherto unrecognized third CDV receptor expressed by glial cells that contributes to the induction of noncytolytic cell-to-cell viral transmission in astrocytes.

IMPORTANCE

While persistent measles virus (MeV) infection induces SSPE in humans, persistent canine distemper virus (CDV) infection causes chronic progressive or relapsing demyelination in carnivores. Common to both central nervous system (CNS) infections is that persistence is based on noncytolytic cell-to-cell spread, which, in the case of CDV, was demonstrated to rely on functional membrane fusion machinery complexes. This inferred a mechanism where nucleocapsids are transmitted through macroscopically invisible microfusion events between infected and target cells. Here, we provide evidence that CDV induces such microfusions in a SLAM- and nectin-4-independent manner, thereby strongly suggesting the existence of a third receptor expressed in glial cells (referred to as GliaR). We propose that GliaR governs intercellular transfer of nucleocapsids and hence contributes to viral persistence in the brain and ensuing demyelinating lesions.

Canine distemper virus (CDV) and measles virus (MeV) belong to the *Morbillivirus* genus of the *Paramyxoviridae* family and induce severe diseases in humans (MeV) and animals (CDV) with high mortality and morbidity. The *Morbillivirus* glycoproteins H and F assemble as a complex on the cellular plasma membrane or on the viral envelope and constitute the viral fusion machinery. While an H tetramer (composed of stalks supporting head domains) interacts with a host cell surface receptor (1, 2), the F trimer fuses the cellular with the viral envelope, the first essential step leading to viral cell entry and spread.

The pathogenesis of CDV infection in animals resembles that of MeV infection in humans in many respects. Indeed, both viruses enter the host through the alveolar macrophages and dendritic cells in the respiratory tract using the CD150/SLAM molecule (3–6). Subsequently, viral amplification and spread throughout the lymphatic tissues occur, and profound immunosuppression is induced (7–10). The second replicative phase in many organs correlates with the expression of PVRL4 (also termed nectin-4, or N4) by epithelial cells (11–14) and leads to typical gastrointestinal, dermatological, and respiratory signs. Viral replication within the respiratory tract eventually leads to contagion through the release of viral particles in the lumina of the airways (8, 13, 15). Finally, both morbilliviruses may invade the central nervous system (CNS), inducing severe neurological diseases by establishing persistent infections (16–19). However, while neurological complications remain rare in the case of MeV infections, they are common in CDV infections (18, 20).

While persistent MeV infection causes subacute sclerosis pan-

Received 5 January 2015 **Accepted** 9 March 2015

Accepted manuscript posted online 18 March 2015

Citation Alves L, Khosravi M, Avila M, Ader-Ebert N, Bringolf F, Zurbriggen A, Vandevelde M, Plattet P. 2015. SLAM- and nectin-4-independent noncytolytic spread of canine distemper virus in astrocytes. J Virol 89:5724–5733. doi:10.1128/JVI.00004-15.

Editor: D. S. Lyles

Address correspondence to Philippe Plattet, philippe.plattet@vetsuisse.unibe.ch.

doi:10.1128/JVI.00004-15

encephalitis (SSPE) in humans, dogs surviving the immunosuppressive stage of the acute disease tend to develop a chronic progressive or relapsing multifocal demyelinating CNS disease, which resembles multiple sclerosis in humans. Importantly, common to measles and distemper, it has been reported that viral persistence and neurological diseases correlate with viral cell-to-cell spread (preferentially in neurons for MeV [21–24] and astrocytes for CDV [18, 25, 26]), allowing the virus to escape immune detection. As suggested in MeV infections of neurons (23, 27), cell-to-cell spread of CDV in the CNS most likely relies on membrane fusion between infected and target astrocytes to establish free passage of viral nucleocapsids. Indeed, we recently found that functional hetero-oligomeric viral H/F complexes, and thus presumably membrane fusion, were required to allow CDV spread in primary astrocytic cultures (25). However, tangible signs of cell-cell fusion, such as syncytium formation, were completely lacking in persistent infections in astrocytic cultures. Such morphological evidence of fusion could be detected only in cultures manipulated to express SLAM, a receptor which is absent in normal CNS cells. Therefore, we predicted that membrane fusion activity may be restricted to the formation of microscopically invisible microfusion pores, which may rely on highly specific conditions, including the involvement of a receptor other than SLAM. This view was further supported by our recent findings showing that the extent of morbillivirus-induced fusion also depends on the nature of the viral receptor (28).

While enormous progress has been made in recent years on the morbillivirus receptors involved in the systemic phase of the infection (8, 16, 29–32), not much has been done on the role of such receptors in the CNS. Our previous report using dog brain cell cultures (DBCCs) revealed that primary astrocytes did not express SLAM (25), thereby arguing against this molecule as a main organizer of viral persistence. In line with this idea, Pratakpiriya and colleagues recently suggested the involvement of canine N4 (cN4) in CDV-mediated neuropathogenesis, based on the fact that some neurons could be stained for both CDV antigens and cN4 (14). These data indicate cN4 as a putative candidate receptor eventually regulating persistent infections.

In this study, we present evidence that cN4 was not expressed in either cultured primary astrocytes or in the white matter of brain sections of infected and noninfected dogs. Interestingly, cN4 expression could be detected in the ependymal cell layer and focally in the meninges. These data, combined with the fact that an engineered recombinant "cN4-blind" neurovirulent CDV retained full cell-to-cell transmission efficacy in primary astrocytes, formally demonstrated that cN4 is not required to support persistent infections. Rather, our findings provide strong evidence for the existence of a third cellular receptor for CDV expressed in glial cells (referred to as GliaR) that may induce microfusion pores, thereby allowing cell-to-cell viral spread and persistence.

MATERIALS AND METHODS

Cell cultures. Primary dog brain cell cultures (DBCCs) were prepared as described elsewhere (26). Subconfluent batches of DBCCs were used for the different experiments and kept at 37°C in the presence of a 5% CO_2 atmosphere. Petri dishes covered with glass coverslips and coated with poly-L-lysine (Sigma-Aldrich, Switzerland) were used for seeding DBCCs for further immunofluorescence assays. The cultures were composed predominantly of astrocytes and were kept alive for up to 3 months. Dulbecco's modified Eagle medium (DMEM; Life Technologies, Zug, Switzerland) supplemented with 10% fetal calf serum (FCS; Bioswisstec, Schaffhausen, Switzerland) and penicillin-streptomycin (Life Technologies) was changed every 2 to 3 days. Vero cells (receptor-negative) and two other Vero cell lines constitutively expressing either the canine SLAM receptor (Vero-cSLAM; kindly provided by Yusuke Yanagi) or the canine nectin-4 receptor (Vero-cN4) (28) were grown in DMEM supplemented with 10% FCS and 1% penicillin-streptomycin and incubated at 37°C in the presence of a 5% CO_2 atmosphere. Vero-cSLAM cells were incubated once a week with Zeocin (Invitrogen, Switzerland).

Viruses. The recombinant A75/17-CDV engineered to express red fluorescent protein (recA75/17^{rfp}) was used in all infection experiments. The virus is derived from the wild-type (wt) demyelinating canine distemper virus A75/17 strain (33) and was exclusively amplified in Vero-cSLAM cells. The recA75/17^{rfp} H^{ko} (where ko is knockout) is a variant which lacks the attachment protein gene. To complement the deficiency, the latter virus was amplified in Vero-cSLAM cells expressing the H protein (Vero-cSLAM-H) cells, as elsewhere described (25). A recombinant A75/17^{rfp} strain bearing a single substitution in the H protein (Y539A) was previously successfully rescued and demonstrated to be unable to infect primary canine keratinocytes (34). recA75/17^{rfp} and recA75/17^{rfp} H-Y539A were amplified and titrated in Vero-cSLAM cells, as previously described (35).

Virus growth kinetics and virus titration assays. Vero, Vero-cSLAM, and Vero-cN4 cells were infected with the recA75/17^{rfp} and the recA75/17^{rfp} H-Y539A viruses at a multiplicity of infection (MOI) of 0.01 (as titrated in Vero-cSLAM cells). After 2 h the medium was replaced by fresh medium, and samples were taken at 12, 24, 36, 48, and 60 h postinfection. The cell-associated viruses were released by two cycles of freezing and thawing of the cellular monolayer. Growth kinetics were also determined in DBCCs. To this aim, confluent cultures were infected with the recA75/17^{rfp} or the recA75/17^{rfp} H-Y539A virus at an MOI of 0.01 (as titrated in Vero-cSLAM cells). Cell-free and cell-associated viruses were harvested at 3, 6, 9, and 12 days postinfection (p.i.). All samples were titrated in Vero-cSLAM cells by limited dilutions as described previously (36).

Cell-cell fusion assay. A fusion assay was performed as described elsewhere (37). Briefly, 6×10^5 Vero, Vero cSLAM, or Vero cN4 cells, plated 24 h prior to the experiment in six-well plates, were cotransfected with 1 μg of either the pCI plasmid expressing the H protein of A75/17 (pCI-H-A75/17, or pCI-H) or the H-Y539A mutant (pCI-H-Y539A) along with 1.8 μg of pCI-F and 0.2 μg of pCI-RFP (expressing the red fluorescent protein). In some experiments, a previously described F variant was coexpressed with H proteins (pCI-F-L372A) (28, 38). All of the pCI-H- and -F-expressing constructs were previously described (28, 34, 38). Cells were visually assessed at 24 h (or as indicated in the text) posttransfection for the presence of syncytia, and represented field of views were captured with an inverted fluorescence microscope (FluoView FV1000; Olympus).

Confocal fluorescence microscopy. Cell-to-cell spread of the recA75/17^{rfp} or the recA75/17^{rfp} H-Y539A virus in Vero, Vero-cSLAM, and Vero-cN4 cells and DBCCs were tracked under real-time conditions by laser scanning confocal fluorescence microscopy (FluoView FV1000; Olympus) because both viruses additionally expressed the red fluorescent reporter protein. Images were monitored at 1, 3, and 5 days p.i. Virus tracking was similarly performed in DBCCs with the difference that images were taken at 3, 6, 9, 12, and 16 days p.i.

Immunofluorescence analysis. DBCCs were plated in petri dishes containing glass coverslips. At the time of infection (0 days p.i.) and 6 weeks postinfection, cells were fixed with 4% phosphate-buffered saline (PBS)-buffered paraformaldehyde for 20 min at room temperature. For intracellular component staining, the coverslips were washed twice with 0.1% Tween 20 in PBS (PBS-T) and permeabilized with 0.1% Triton X-100 (Sigma-Aldrich, Switzerland) for 5 min. For cell surface component staining, cells were not permeabilized. After two washes with PBS-T, cells were blocked for 1 h at room temperature with PBS-T containing 10% of either normal goat serum (Dako, Baar, Switzerland) or fetal calf serum. The first antibodies were diluted in PBS-T and incubated at room temperature overnight in a humid atmosphere. Coverslips were then

washed three times in PBS-T, and the appropriate Alexa Fluor-conjugated secondary antibodies (1:500 in PBS-T) were incubated at room temperature for 1 h together with 4′,6-diamidino-2-phenylindole ([DAPI] D1306; Life Technologies) for nucleus counterstaining (1:10,000 in PBS-T). Finally, the cells were washed twice in PBS-T and once in distilled water and subsequently mounted on glass slides with Glycergel (Dako Diagnostics, Zug, Switzerland). Slides were then monitored by laser scanning confocal microscopy (FluoView FV1000 software; Olympus).

Immunohistochemistry. Histological paraffin sections of dog tissues were used for detection and distribution analysis of nectin-4, including brain, trachea, and small intestine. Tissue sections were deparaffinized and rehydrated following standard immunohistochemistry protocols. After endogenous peroxidase was quenched with 3% H_2O_2 in PBS-T for 15 min, the tissues were submitted to heat-induced epitope retrieval at 95°C for 20 min. The slides were cooled down, washed three times in PBS-T, and subsequently blocked with 5% FCS in PBS-T over 20 min. Next, tissue sections were incubated overnight at 4°C with the first polyclonal antibody, anti-nectin-4 (AF2659; R&D Systems) at a concentration of 1:1,000 in PBS-T under a humid atmosphere. Successively, biotinylated donkey anti-goat secondary antibody (1:1,000 in PBS-T) (705-065-003; Jackson ImmunoResearch) and peroxidase-labeled streptavidin conjugate (1:1,000 in PBS-T) (016-030-084; Jackson ImmunoResearch) were added for 30 min each at room temperature in the dark. Finally, the slides were treated with 3,3″-diaminobenzidine substrate (AEC kit 101-1KT; Sigma-Aldrich, Switzerland) and counterstained with Ehrlich's hematoxylin for 6 s. Slides were washed twice in PBS-T, rinsed with distilled water, and mounted on glass slides with Aquatex (Dako Diagnostics, Zug, Switzerland).

Antibodies. Several antibodies were used for the investigation of cellular components: mouse monoclonal antibody (MAb) anti-glial fibrillary acidic protein (GFAP; 1:1,000) (ab4648; Abcam, Switzerland), rabbit polyclonal antibody anti-GFAP (1:1,000) (Z0334; Dako Diagnostics, Zug, Switzerland), mouse monoclonal antibody anti-vimentin (1:1,000) (M7020; Dako Diagnostics, Zug, Switzerland), mouse monoclonal antibody anti-neurofilament II (1:200) (C0762; Dako Diagnostics, Zug, Switzerland), and goat polyclonal antibody anti-human nectin-4 (1:1,000) (AF2659; R&D Systems). The fluorescently labeled secondary antibodies used were Alexa Fluor 488 goat anti-rabbit IgG (1:500) (A11008; Life Technologies), Alexa Fluor 488 and 647 goat anti-mouse IgG (each, 1:500) (A-11001 and A-21235, respectively; Life Technologies), and Alexa Fluor 488 and 647 donkey anti-goat (each, 1:500) (A-11055 and A-21447, respectively; Life Technologies).

Reverse transcription-PCR (RT-PCR). Total RNA was isolated from uninfected and infected DBCCs and from Vero, Vero-cSLAM, and Vero-cN4 cell cultures using an RNeasy kit (Qiagen AG, Basel, Switzerland) and reverse transcribed into cDNA using Superscript III reverse transcriptase and random primers (SuperScript III First-Strand Synthesis SuperMix, 18080-400; Life Technologies). Specific DNA sequences were amplified using a high-fidelity polymerase-containing kit (HiFidelity PCR kit; Qiagen). Amplicons were then run on a 1.5% agarose gel and visualized with a UV camera (Quantum ST5-1100/26LMX X-Press; Vilber Lourmat, Witec AG, Switzerland) with the Quantum ST5 X-Press software package. Specific primers for amplifying the housekeeping gene glyceraldehyde-3-phosphate dehydrogenase (GAPDH) were used as internal controls. All primers employed for the PCRs are available upon request.

Sequencing of the H-A75/17 gene. Viral RNAs from 6-week-old infected DBCCs were extracted, reverse transcribed, and amplified as described above, with the difference that primers specific for the amplification of the H-A75/17 gene were employed (available upon request). Subsequently, the DNA products were sequenced using a BigDye, version 3.1, cycle sequencing kit (43374; Life Technologies). The sequencing reactions were run on an ABI 3730 automated sequencer.

RESULTS

The cN4 molecule is not expressed at detectable levels in DBCCs. Since some CDV-positive neurons additionally exhibiting cN4 expression could be detected in infected canine brains, Pratakpiriya and colleagues proposed a role of cN4 in CDV neuropathogenesis (14). However, no clear data were provided regarding cN4 expression in astrocytes, the main target cells sustaining viral persistence in the brain. With the aim to determine whether cN4 might play a role in persistent CDV infections, we first used dog brain cell cultures (DBCCs) to evaluate the level of cN4 expression in glial cells. As previously reported (25, 26), we confirmed (i) that DBCCs were mainly composed of astrocytes and (ii) that A75/17-CDV spread in this cell system from cell to cell in a noncytolytic manner with extremely small amount of free particle production (not shown).

To investigate the presence of cN4 in astrocytes at the protein and RNA levels, we performed immunostainings and RT-PCR analyses, respectively. Because no anti-canine N4 antibody is currently available, immunofluorescence (IF) analyses were performed using a polyclonal anti-human N4 antibody (cross-reacting with the canine N4 molecule). IF did not reveal any staining in primary astrocytes regardless of whether the cells were infected (Fig. 1A, left panel) or not (data not shown). As controls, Vero and Vero-cN4 cells were also stained with the polyclonal antibody, and fluorescence emission could be detected only in Vero-cN4 cells (Fig. 1A, right panel).

To further confirm these results, total RNA was initially extracted from Vero, Vero-cSLAM, and Vero-cN4 cells, and selective amplification of the desired receptor was validated using specific sets of primers. Primers designed to amplify the GAPDH gene were also included in this set of experiments and served as internal controls for the assay (Fig. 1B). Next, RT-PCRs were repeated from total RNA extracted from infected DBCCs; the experiment shown in Fig. 1B indicates that after 35 cycles of amplification neither cSLAM nor cN4 could be detected, whereas the GAPDH and CDV H genes were readily amplified. Lack of detection of both receptors' mRNAs was also obtained from noninfected DBCCs (data not shown).

Taken together, these data strongly suggested that both known morbillivirus receptors, cN4 and cSLAM, were not expressed to detectable levels in primary astrocytes. Consequently, these findings further indicated that persistent CDV infections (which are promoted by functional viral fusion machineries [25]) relied on a mechanism that did not require the presence of a cell surface receptor that triggers membrane fusion through H contacts (akin the proposed cell-to-cell spread of MeV in neurons [23]). Alternatively, a yet unidentified (H-binding) CDV receptor expressed in glial cells may contribute to persistent infections by inducing highly restricted membrane fusion activity.

cN4 remains undetectable in the white matter of dog brain tissues. In order to explore whether our *in vitro* findings may corroborate the *in vivo* situation, we next determined the cN4 expression pattern in the brain of adult dogs. To this purpose, we selected tissue sections from uninfected adult dogs and from A75/17-CDV-infected ones that exhibited chronic encephalitis.

Immunohistochemical staining of paraffin-embedded tissue sections was thus performed using the anti-human N4 polyclonal antibody. Representative micrographs and close-up insets of cN4 distribution are presented in Fig. 2. As controls, paraffin sections

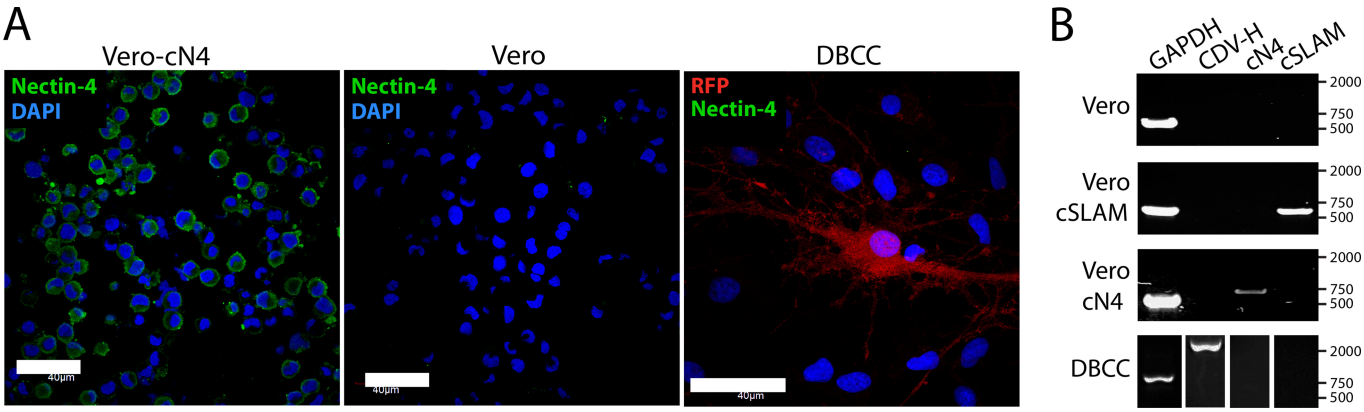

FIG 1 The morbillivirus cellular receptor cN4 is not expressed in DBCCs. (A) Noninfected Vero-cN4 cells and regular Vero cells as well as noninfected (not shown) and infected DBCCs were stained with an anti-human nectin-4 antibody. Immunofluorescence analyses indicated a clear signal exclusively in cells expressing nectin-4. Representative fields of view were pictured using an inverted confocal fluorescence microscope (magnification, ×100; FluoView FV1000; Olympus). (B) cN4 mRNA is not detected in noninfected (not shown) or infected DBCCs. Total RNA was extracted from noninfected Vero, Vero-cSLAM, and Vero-cN4 cells as well as from infected DBCCs and subjected to RT-PCRs to investigate the expression of the housekeeping gene GAPDH and the A75/17 H (CDV H), cN4, and cSLAM genes.

of dogs' intestinal tissues were included. Clear positive immunostaining with a basolateral distribution pattern in enterocytes was detected, which is entirely consistent with the expected localization of N4 in the zonula adherens (Fig. 2A).

In transversal sections of cerebellum and brainstem, only weak and inconsistent punctate cN4 staining was detected in some large brainstem neurons of both infected and uninfected CNSs. Importantly, there was no consistent staining detected in the white matter (Fig. 2B). Interestingly, positive immunostaining could be observed in the ependymal cell layer and, perhaps, multifocally in meningeal elements (Fig. 2C). The ependymal staining was mostly restricted to the surface facing the ventricle, including the cilia.

In sum, while cN4 expression in ependymal cells must be validated using canine-specific reagents, these data nevertheless suggested that cN4 is very likely not critical in supporting efficient persistent CDV infections in both primary astrocytes and white matter of canine brains.

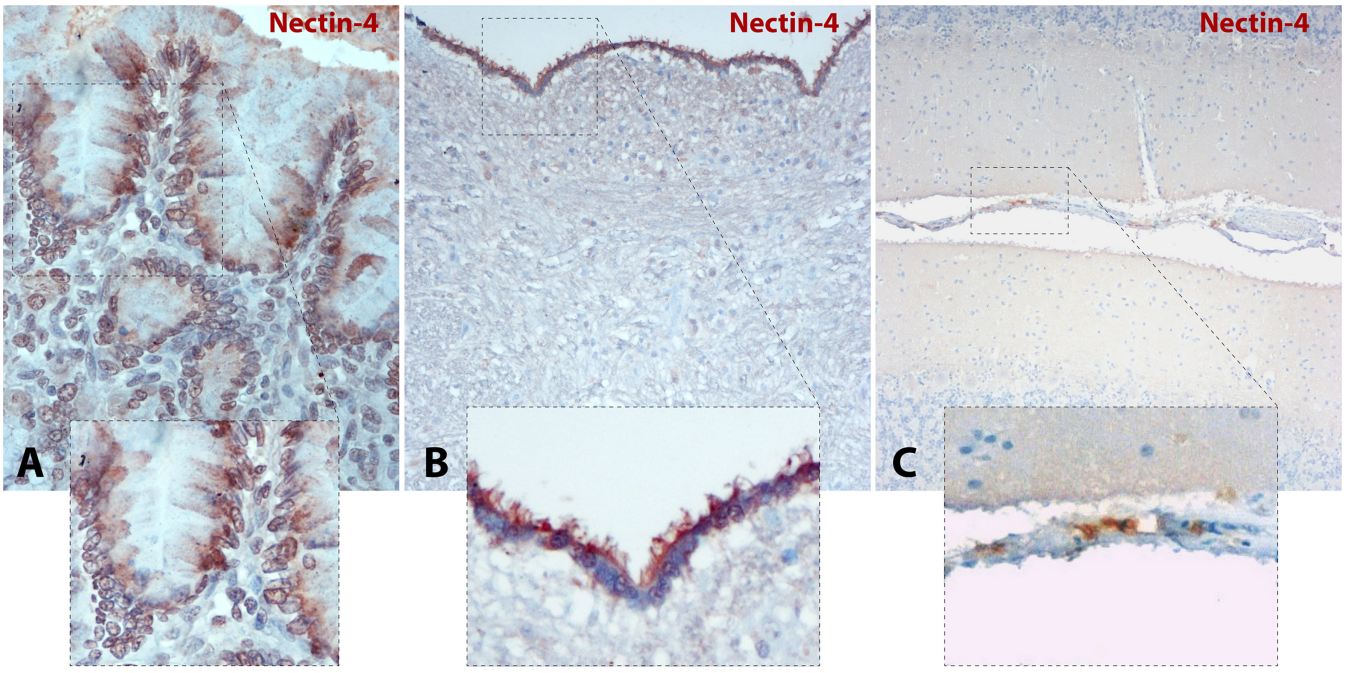

FIG 2 Nectin-4 is not detected in dog brain parenchyma. (A) Canine N4 staining from a paraffin section of intestine revealed N4 expression at the basolateral side of enterocytes. A close-up view of the selected area is shown in the inset. (B) Canine N4 staining from a brainstem paraffin section at the level of the medulla oblongata, fourth ventricle floor (IV), indicated the absence of N4 expression. Conversely, positive cN4 staining was found in the ependymal cell layer. A close-up view of the ependymal cell layer is shown in the inset. (C) Canine N4 staining from a cerebellum paraffin section confirms the absence of N4 with some exceptions in the meninges. A close-up view of the cerebellar leptomeninges with slight positive N4 staining is shown in the inset. Photomicrographs were taken at a magnification of ×400.

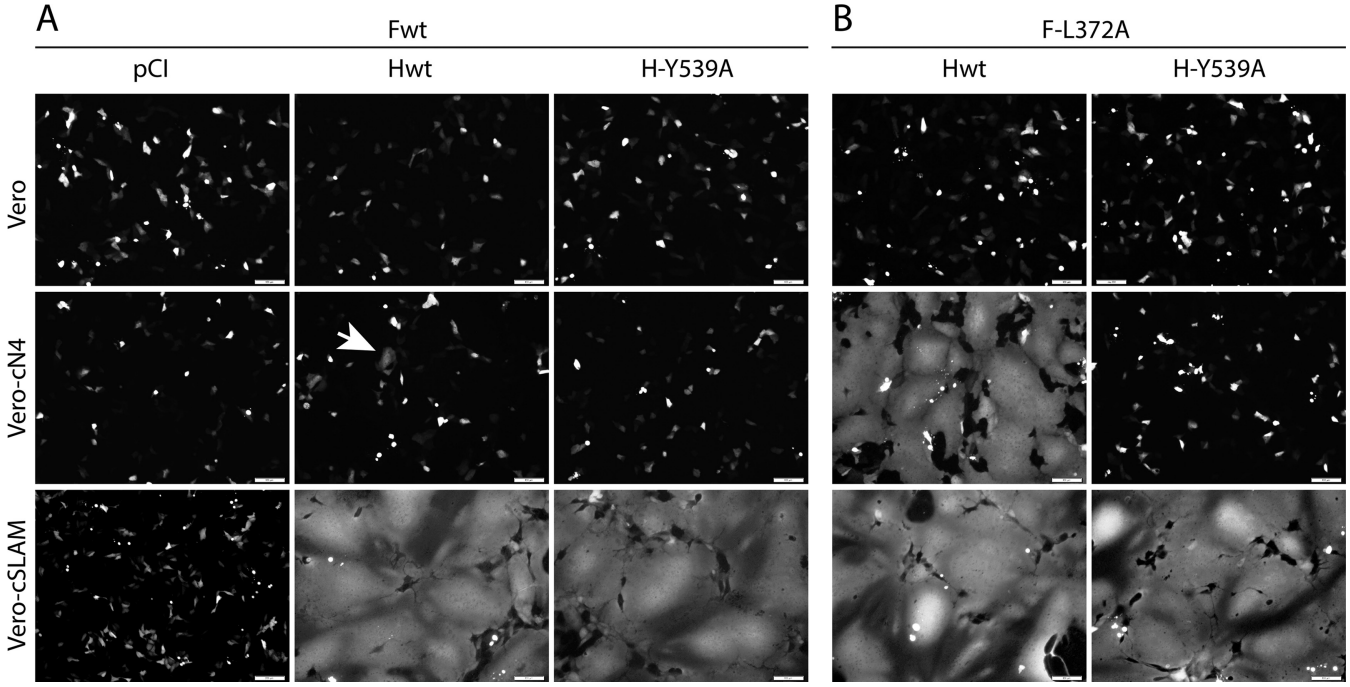

FIG 3 Cell-cell fusion efficacy in the presence of canine N4 of H-A75/17 and derivative H-Y539A mutant viruses. Vero, Vero-cN4, and Vero-cSLAM cells were transfected with DNA plasmids encoding empty vector (pCI), H-A75/17 (Hwt), or H-Y539A along with F-A75/17 (Fwt) (A) or F-L372A (B). A plasmid encoding the red fluorescent protein was included to increase the sensitivity of the assay. Representative fields of view were captured at 24 h (or 48 h for the Hwt and F-L372A combination in Vero-cN4 cells) posttransfection with a confocal microscope (magnification, ×100; FluoView FV1000; Olympus). The white arrow indicates very limited induction of cell-cell fusion.

A single substitution in H (H-Y539A) ablates bioactivity selectively through cN4. Although immunostaining and RT-PCR technologies failed to record cN4 expression in primary astrocytic cultures, the sensitivity of both methods might have missed the detection of minute amounts of cN4 expression. In fact, extremely low production of cN4 in astrocytes may account for the proposed microfusion pore induction and ensuing free transfer of nucleocapsids. We thus thought to employ a virus-based, highly sensitive system to explore this possibility. We previously reported that A75/17-CDV induced only very limited syncytia in primary canine epithelial keratinocyte cultures and identified a mutation in the H protein (H-Y539A) which fully ablated the capacity of the virus to infect these cells (34). Later on, N4 was discovered as an entry receptor for morbilliviruses in epithelial cells (11–14). Consistent with the idea that cN4 may contribute to the limited membrane fusion activity mediated by A75/17 in keratinocytes, we recently provided evidence that cell-cell fusion in Vero cells expressing cN4 remained, indeed, scarcely activated (28).

To validate the role of the H variant (Y539A) in ablating membrane fusion selectively through cN4, we performed cell-cell fusion assays in Vero cells expressing, or not, a morbillivirus receptor (cSLAM and cN4) by transfecting different combinations of CDV glycoproteins. As expected, while massive membrane fusion was triggered though the SLAM receptor with standard H and F proteins, the activity remained only marginal in the presence of cN4 (Fig. 3A, central panels). When H-Y539 was coexpressed with F-wt, fusion was selectively recorded in Vero-cSLAM cells (Fig. 3A, right panels). We then repeated the experiments using a reported destabilized F mutant which strongly enhances bioactivity (F-L372A) (28). Under these experimental settings, massive syncytium formation was observed when H-wt and F-L372A were expressed in Vero cells expressing one or the other receptor (Fig. 3B, left panels). Conversely, the H-Y539A/F-L372A combination triggered membrane fusion selectively in the presence of cSLAM (Fig. 3B, right panels).

These results taken together demonstrated that, similar to the analogous MeV H-Y543A mutant (31), CDV H-Y539A is completely deficient in mediating fusion via cN4 (even in the presence of a destabilized F mutant) even though there is a productive interaction with cSLAM.

A recombinant A75/17 virus carrying the H-Y539A substitution is growth defective in Vero-cN4 cells. To investigate whether the data obtained in transient-transfection assays could be recapitulated in the context of full viruses, we infected the three Vero cell lines with recA75/17^{rfp} and recA75/17^{rfp} H-Y539A and monitored their patterns of infectivity and spread using fluorescence microscopy over a period of 5 days. As expected, both viruses demonstrated very slight levels of infection and spread in Vero cells, whereas they induced massive fusion in the presence of cSLAM (Fig. 4A and B). Strikingly, while recA75/17^{rfp} could also induce syncytia in Vero-cN4 cells, recA75/17^{rfp} H-Y539A activity in Vero-cN4 cells was not significantly different from that in Vero cells (Fig. 4A and B). Of note, and supporting the results of the transient-transfection experiments, membrane fusion activity induced by recA75/17^{rfp} in the presence of cN4 was much less pronounced than that induced in the presence of cSLAM (Fig. 4A).

We finally determined the growth kinetics of both viruses in the various cell lines. Consistent with the infection pattern, recA75/17^{rfp} hardly replicated in Vero cells, whereas titers of about 10^6 infectious units/ml were reached in Vero-cSLAM cells

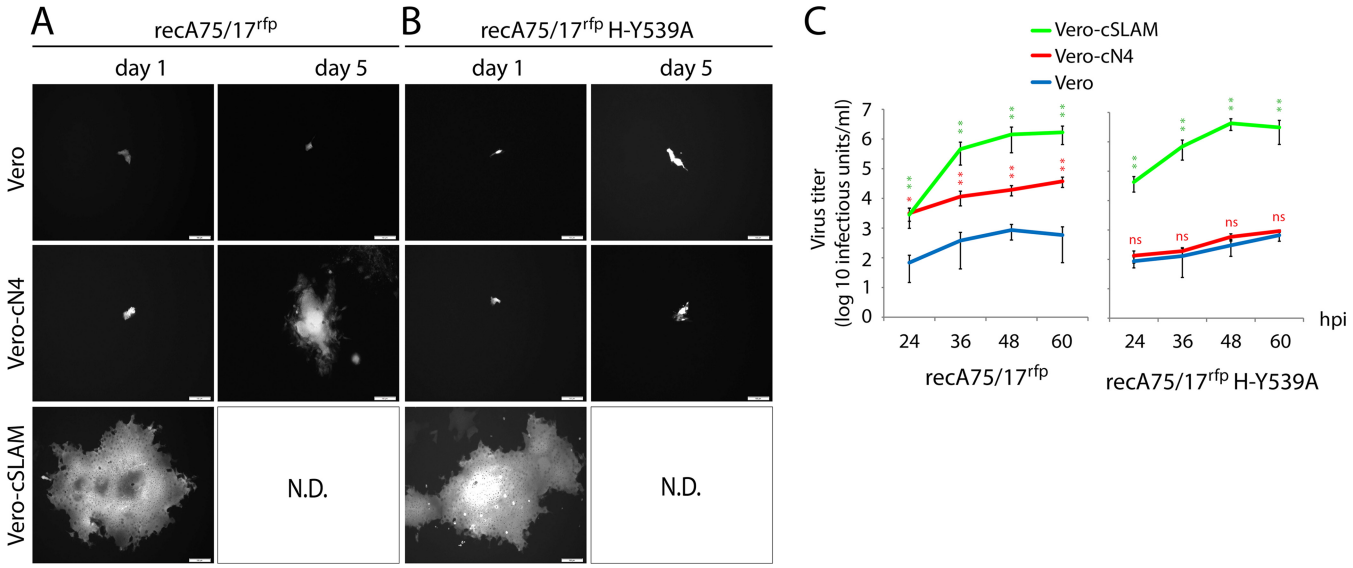

FIG 4 Receptor-dependent differences in recA75/17^{rfp} and recA75/17^{rfp} H-Y539A infection profiles. (A and B) Vero, Vero-cN4, and Vero-cSLAM cells were infected with recA75/17^{rfp} or recA75/17^{rfp} H-Y539A at an MOI of 0.01. Representative fields of view were captured at 1, 3, and 5 days postinfection with a confocal microscope (magnification, ×100; FluoView FV1000; Olympus). ND, not determined (because the cell culture was fully lysed). (C) Growth curves of wt and cN4^{blind} viruses in different cell lines. recA75/17^{rfp} and recA75/17^{rfp} H-Y539A (renamed recA75/17^{rfp} H-cN4^{blind}) growth curves were obtained by infection of Vero, Vero-cSLAM, and Vero-cN4 cells at an MOI of 0.01. Cell-associated viruses were harvested at 0, 12, 24, 36, 48, and 60 h postinfection (hpi), and titration experiments were performed in Vero-cSLAM cells. Means ± standard deviations of data from three independent experiments performed in triplicates are shown. To determine the statistical significance of differences between the wt and the mutant viruses' data sets, unpaired two-tailed *t* tests were performed (*, $P < 0.05$; **$P < 0.01$; NS, not significant).

already at 36 h postinfection (Fig. 4C). In contrast, in Vero-cN4 cells, the wt virus grew much more slowly and reached lower titers since only 10^4 infectious units/ml was recorded at 60 h p.i. (Fig. 4C). Importantly, recA75/17^{rfp} H-Y539A did not exhibit any growth advantage in Vero-cN4 cells compared to its growth in Vero cells while it reached wt-like titers in the presence of cSLAM (Fig. 4C).

Altogether, these results formally demonstrated (i) that cN4 acted as a functional cellular receptor for the prototypic neurovirulent and demyelinating A75/17-CDV strain and (ii) that the Y539A substitution in the attachment protein specifically caused the loss of fusion triggering through the cN4 receptor. We therefore renamed the recA75/17^{rfp} H-Y539A virus recA75/17^{rfp} H-cN4^{blind}.

recA75/17^{rfp} H-cN4^{blind} exhibits noncytolytic cell-to-cell transmission efficacy in primary dog brain cell cultures. The reprogrammed recA75/17^{rfp} H-cN4^{blind} virus offered an ideal molecular tool to investigate, in a highly sensitive manner, the role of cN4 in controlling A75/17-mediated noncytolytic cell-to-cell transmission in primary brain cell cultures. We thus inoculated the wild-type and the engineered cN4^{blind} viruses in the astrocytic cell culture system and monitored their transmission ability using live-cell fluorescence microscopy.

Remarkably, in primary astrocytes, the kinetics and mode of transmission of recA75/17^{rfp} H-cN4^{blind} were very similar to the infection profile mediated by recA75/17^{rfp} (Fig. 5A and B). Infected cells did not exhibit any signs of fusion and/or cytolysis, and long fluorescent astrocytic processes were often observed bridging neighboring infected foci. Thus, cell-to-cell transmission with recA75/17^{rfp} H-cN4^{blind} remained typically noncytolytic. Of note, these specific infection profiles were preserved even 6 weeks postinoculation for both the wild-type and the mutant viruses (data not shown).

To further confirm that the cN4^{blind} virus indeed exhibits properties similar to those of its wild-type counterpart, we verified its ability to produce free particles. Growth kinetics of cell-associated and cell-free viruses were thus determined throughout a period of 12 days. Titers of cell-associated viruses recorded for both viruses displayed very similar kinetics and were reaching identically low values at 12 days postinoculation (slightly more than 10^2 infectious units/ml) (Fig. 5C). The deficiency was even more marked regarding virus budding since titration experiments of cell-free particles revealed the absence, or an extremely small amount, of free viruses released in the supernatant for both viruses (Fig. 5D). We thus concluded from this set of experiments that the efficient dissemination of recA75/17^{rfp} H-cN4^{blind} in primary astrocytes did not rely on extracellular particle formation but, rather, on a unique intercellular cell-to-cell mechanism.

Because RNA viruses contain polymerases with high mutational rates (indicating their ability to swiftly react to any environmental selective pressures by introducing adaptive mutations in the viral genome) (39), we assessed whether the efficient spread in astrocytes monitored with the cN4^{blind} virus correlated with a reversion of the single substitution introduced in the wild-type sequence. To this aim, total RNA was extracted from 6-week-old persistently infected cell monolayers, followed by RT-PCRs. Sequencing analysis of the products indicated that the H gene (of two independent infections) of either the wild-type or the cN4^{blind} virus remained unaltered. Indeed, both viruses unequivocally conserved their original H predicted amino acid sequences with the tyrosine and the alanine at position 539 of the wild-type and mutant viruses, respectively (data not shown).

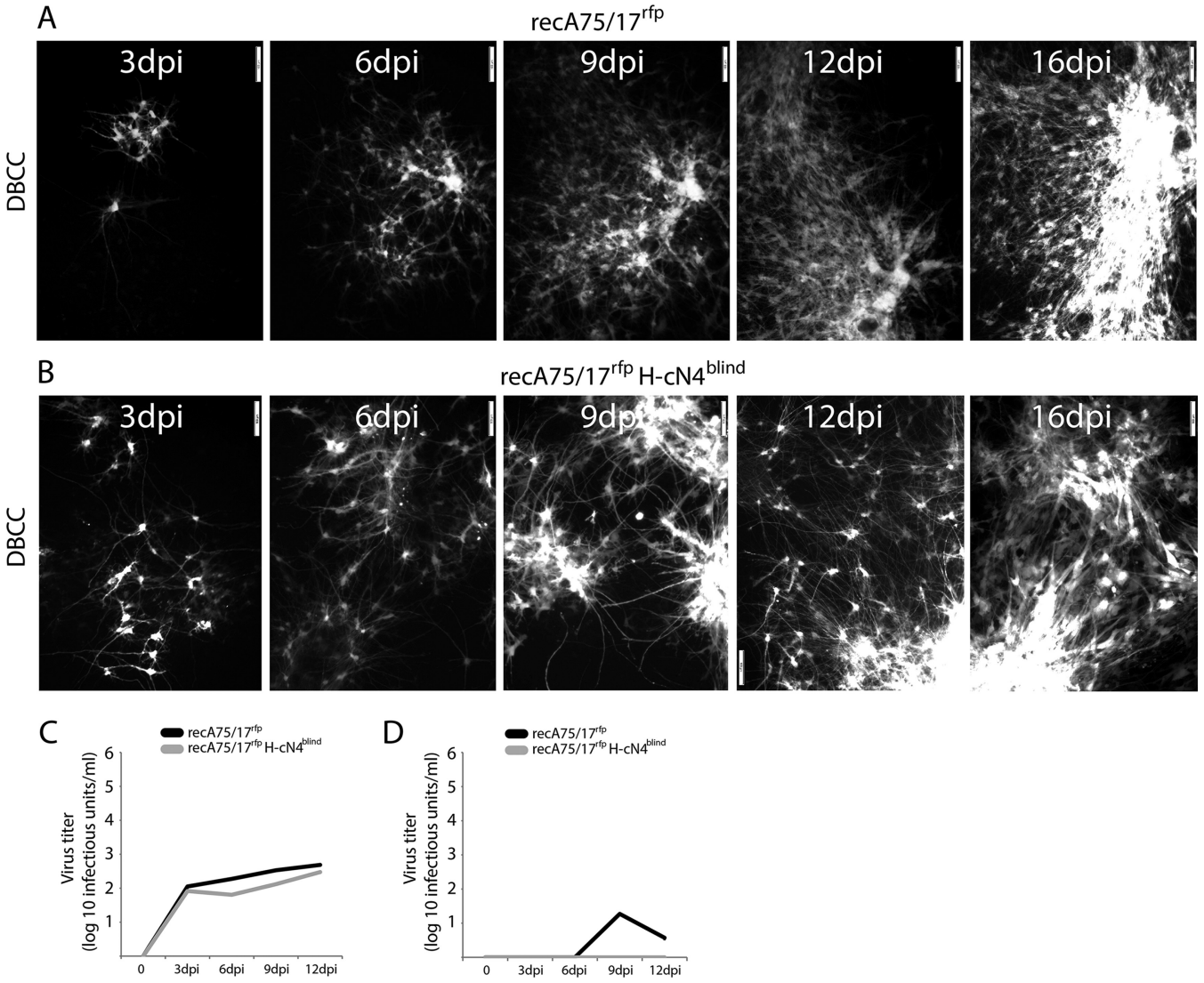

FIG 5 Efficacy of recA75/17^{rfp} and recA75/17^{rfp} H-cN4^{blind} cell-to-cell transmission in DBCCs. (A and B) Cell-to-cell spread of recA75/17^{rfp} or recA75/17^{rfp} H-cN4^{blind} in DBCCs was monitored throughout a period of 16 days. Cell-to-cell transmission in living cells was performed by recording virus-induced red fluorescence emission. In both experiments representative fields of growing infected foci were captured at 3, 6, 9, 12, and 16 days postinfection (dpi) with a confocal microscope (magnification, ×100; FluoView FV1000; Olympus). (C and D) Both recA75/17^{rfp} and recA75/17^{rfp} H-cN4^{blind} are defective in producing free particles in DBCCs. Growth kinetics in DBCCs of cell-associated (C) or cell-free (D) particles generated by recA75/17^{rfp} or recA75/17^{rfp} H-cN4^{blind} were determined. DBCCs were infected with the both viruses at an MOI of 0.01, and particles in the supernatant or remaining bound to the cells were harvested at 0, 3, 6, 9, and 12 days postinfection. Results represent the means of three independent experiments. To determine the statistical significance of differences between the growth of the wt virus (or cN4^{blind} mutant) in Vero cells expressing the indicated receptor compared to its growth in regular Vero cells, unpaired two-tailed *t* tests were performed (*, $P < 0.05$; **$P < 0.01$).

Collectively, these findings provided supplementary key evidence that cN4 is not involved in regulating cell-to-cell virus spread in primary astrocytes while further supporting the notion that CDV persistence in the white matter of canine brains also does not rely on cN4.

DISCUSSION

Neurological complications in MeV and CDV infections result from viral persistence, which is based on viral cell-to-cell spread through neurons in SSPE (21, 22, 24) and through astrocytes in demyelinating distemper encephalitis (25). Although direct evidence remains elusive, in both MeV and CDV brain infections, virus transfer is thought to occur through microfusions between infected and target cells (21, 25, 40). Importantly, transmission deficiency of an H^{ko} recombinant CDV (25) combined with the finding that an anti-H monoclonal anybody (1347) (25) as well as a small-molecule F refolding-blocker (3g) (41) efficiently inhibited viral spread strongly suggested that the putative microfusion events require functional viral membrane fusion machineries.

Currently, two morbillivirus receptors have been identified: SLAM in lymphatic tissues and N4 in epithelial tissues (3, 4, 11–14), explaining pathological consequences such as immunosuppression, and respiratory and gastrointestinal lesions. Although neuro-invasion may also require the expression of appropriate viral receptor(s)

in neural cells, the role of viral receptors in neurological complications of morbillivirus infections has received much less attention. In CDV infections, there is little evidence that cSLAM may be involved in neuropathogenesis since cSLAM is not constitutively expressed in the canine brain (42) and since we failed to detect cSLAM RNA expression in primary astrocytic cultures (25). In contrast, because Pratakpiriya and colleagues recently demonstrated the presence of canine N4-positive CDV-infected neurons, a putative role of cN4 in CDV neuropathogenesis was inferred (14).

Our initial findings were in favor of the assumption that cN4 could be responsible for persistent infections in the white matter (25, 43, 44). Indeed, cell-cell fusion induced by A75/17 was dramatically less pronounced in Vero-cN4 than in Vero-cSLAM cells. However, essential pieces of evidence further supporting this notion were lacking: we were unable to demonstrate expression of cN4 in the white matter on tissue sections as well as in cultured canine astrocytes. Moreover, and unexpectedly, a $cN4^{blind}$ virus replicated and spread very efficiently in primary astrocytic cultures. Having additionally excluded the possibility of reversion to the wild-type sequence of the single amino acid substitution carried by the $cN4^{blind}$ virus and considering the findings of previous studies (25, 41), we hypothesize that persistent infection of virulent CDV in the CNS white matter is dependent on a third hitherto unknown receptor expressed by glial cells.

However, in analogy to persistent MeV infections in neurons, an alternative explanation would be cell-to-cell transmission exclusively relying on the viral fusion protein without the support of H. Previous results suggested that the initial entry of MeV relied on the presence of a receptor, whereas subsequent nucleocapsid transfer at synaptic contacts might not (23). Indeed, it has been proposed that F alone could bind to a specific receptor, resulting in the activation of the membrane fusion process (23). Consistent with the latter hypothesis, our latest results indeed indicated that F complexes efficiently trafficked to the cell surface in their bioactive prefusion, metastable state even in the absence of H (45). However, if F trimers alone could truly trigger fusion in the absence of H, why did the H^{ko} recombinant virus exhibit deficiency in cell-to-cell transmission?

Molecular characterization of the MAb anti-CDV-H 1347 provides additional arguments against the concept of CDV F being able to induce membrane fusion on its own. Indeed, we found that MAb 1347, which efficiently blocks nucleocapsid transfer in astrocytes (25), binds to the stalk region of H and blocks fusion promotion without interfering with either receptor interaction or F-H binding activity (unpublished data). Therefore, these findings argue against two alternative hypotheses: (i) H-receptor contact merely shortens the distance between the two opposite membranes, in turn allowing F to refold in an H-independent manner, or (ii) H is responsible for transporting F in selective plasma membrane microdomains where it can engage its own receptor. Thus, our data taken together invariably indicated that persistent infections relied on fully functional H and F proteins, which provided multiple lines of evidence that noncytolytic cell-to-cell transmission can be best explained by the existence of a third receptor expressed by glial cells (GliaR).

Collectively, our *in vitro* and *in vivo* data allowed us to propose a model sustaining CDV neuro-invasion and ensuing immunopathological complications. Following primary replication of CDV in the lymphatic tissues, which is mediated by the SLAM receptor, further dissemination of the infection to the epithelial organs is dependent on N4 (8, 11–13, 31, 46). The putative GliaR expressed in perivascular astrocytes could be accessed either from infected endothelial cells or from CDV-carrying circulating mononuclear cells, which have been shown to penetrate the blood-brain barrier (47). Alternatively, based on positive immunostaining, we speculate that CDV may also use N4 to breach the ependymal and meningeal barriers, which are, throughout the CNS, in intimate contact with an underlying astroglial cell layer (*glia limitans*). This view might be consistent with the reported frequent periventricular and subpial localization of CDV-induced demyelinating lesions (20, 46, 47) with intense infection of the ependymal cells. Once astrocytes are targeted, the infection will further spread deeply in the white matter in a GliaR-dependent manner. Several hypotheses may then explain the ensuing persistent viral infection: (i) selective distribution of GliaR and/or viral fusion machineries at specific microdomains of astrocytic plasma membranes, (ii) suboptimal affinity binding between GliaR and CDV-H, (iii) restricted GliaR expression, (iv) high intrinsic prefusion F stability of wt CDV strains (45), or (v) a combination of these factors (thus opening a narrow F "triggering range," as previously suggested [28]). In turn, these mechanisms will translate into microfusions, with noncytolytic transfer of nucleocapsids at specific contacting sites of neighboring astrocytes, akin to the transsynaptic spread proposed for MeV in neurons. In this way, CDV will swiftly spread in the astrocytic network, thereby outrunning the intrathecal immune response. Consequently, immune reactions keep lagging behind viral replication, which continually creates additional infected foci that, in turn, will be the basis for triggering new cycles of bystander demyelination (25).

In conclusion, while SLAM and N4 have been shown to be essential to understanding the pathogenesis of systemic dissemination in morbillivirus infections, we believe that our model involving a third receptor mediating intercellular viral nucleocapsid transfer in brain cells could help to explain morbillivirus-induced neurological diseases in general. We are thus convinced that identifying GliaR will represent a major breakthrough toward our molecular understanding of morbillivirus neuropathogenesis and possible therapeutic options.

ACKNOWLEDGMENTS

We are grateful to Yusuke Yanagi for having provided the Vero-cSLAM cells.

This work was supported by the Swiss National Science Foundation (reference number 310030_153281 to P.P.), the Novartis Foundation for Biomedical Research (reference number 14A08 to P.P.), and the Berne University Research Foundation (reference number 14/2014 to P.P.).

REFERENCES

1. **Plattet P, Plemper RK.** 2013. Envelope protein dynamics in paramyxovirus entry. mBio **4**(4):e00413-13. http://dx.doi.org/10.1128/mBio.00413-13.
2. **Brindley MA, Plemper RK.** 2010. Blue native PAGE and biomolecular complementation reveal a tetrameric or higher-order oligomer organization of the physiological measles virus attachment protein H. J Virol **84:** 12174–12184. http://dx.doi.org/10.1128/JVI.01222-10.
3. **Tatsuo H, Ono N, Tanaka K, Yanagi Y.** 2000. SLAM (CDw150) is a cellular receptor for measles virus. Nature **406:**893–897. http://dx.doi.org/10.1038/35022579.
4. **Tatsuo H, Ono N, Yanagi Y.** 2001. Morbilliviruses use signaling lymphocyte activation molecules (CD150) as cellular receptors. J Virol **75:**5842–5850. http://dx.doi.org/10.1128/JVI.75.13.5842-5850.2001.
5. **Leonard VH, Hodge G, Reyes-Del VJ, McChesney MB, Cattaneo R.** 2010. Measles virus selectively blind to signaling lymphocytic activation

molecule (SLAM; CD150) is attenuated and induces strong adaptive immune responses in rhesus monkeys. J Virol **84:**3413–3420. http://dx.doi.org/10.1128/JVI.02304-09.

6. **de Swart RL, Ludlow M, de WL, Yanagi Y, van AG, McQuaid S, Yuksel S, Geijtenbeek TB, Duprex WP, Osterhaus AD.** 2007. Predominant infection of CD150$^+$ lymphocytes and dendritic cells during measles virus infection of macaques. PLoS Pathog **3:**e178. http://dx.doi.org/10.1371/journal.ppat.0030178.
7. **Schneider-Schaulies J, Schneider-Schaulies S.** 2008. Receptor interactions, tropism, and mechanisms involved in morbillivirus-induced immunomodulation. Adv Virus Res **71:**173–205. http://dx.doi.org/10.1016/S0065-3527(08)00004-3.
8. **Frenzke M, Sawatsky B, Wong XX, Delpeut S, Mateo M, Cattaneo R, von Messling V.** 2013. Nectin-4-dependent measles virus spread to the cynomolgus monkey tracheal epithelium: role of infected immune cells infiltrating the lamina propria. J Virol **87:**2526–2534. http://dx.doi.org/10.1128/JVI.03037-12.
9. **de Vries RD, McQuaid S, van AG, Yuksel S, Verburgh RJ, Osterhaus AD, Duprex WP, de Swart RL.** 2012. Measles immune suppression: lessons from the macaque model. PLoS Pathog **8:**e1002885. http://dx.doi.org/10.1371/journal.ppat.1002885.
10. **de Vries RD, Lemon K, Ludlow M, McQuaid S, Yuksel S, van Amerongen G, Rennick LJ, Rima BK, Osterhaus AD, de Swart RL, Duprex WP.** 2010. In vivo tropism of attenuated and pathogenic measles virus expressing green fluorescent protein in macaques. J Virol **84:**4714–4724. http://dx.doi.org/10.1128/JVI.02633-09.
11. **Noyce RS, Bondre DG, Ha MN, Lin LT, Sisson G, Tsao MS, Richardson CD.** 2011. Tumor cell marker PVRL4 (nectin 4) is an epithelial cell receptor for measles virus. PLoS Pathog **7:**e1002240. http://dx.doi.org/10.1371/journal.ppat.1002240.
12. **Noyce RS, Delpeut S, Richardson CD.** 2013. Dog nectin-4 is an epithelial cell receptor for canine distemper virus that facilitates virus entry and syncytia formation. Virology **436:**210–220. http://dx.doi.org/10.1016/j.virol.2012.11.011.
13. **Muhlebach MD, Mateo M, Sinn PL, Prufer S, Uhlig KM, Leonard VH, Navaratnarajah CK, Frenzke M, Wong XX, Sawatsky B, Ramachandran S, McCray PB, Jr, Cichutek K, von Messling V, Lopez M, Cattaneo R.** 2011. Adherens junction protein nectin-4 is the epithelial receptor for measles virus. Nature **480:**530–533. http://dx.doi.org/10.1038/nature10639.
14. **Pratakpiriya W, Seki F, Otsuki N, Sakai K, Fukuhara H, Katamoto H, Hirai T, Maenaka K, Techangamsuwan S, Lan NT, Takeda M, Yamaguchi R.** 2012. Nectin4 is an epithelial cell receptor for canine distemper virus and involved in neurovirulence. J Virol **86:**10207–10210. http://dx.doi.org/10.1128/JVI.00824-12.
15. **Racaniello V.** 2011. Virology. An exit strategy for measles virus. Science **334:**1650–1651. http://dx.doi.org/10.1126/science.1217378.
16. **Ludlow M, McQuaid S, Milner D, Swart RL, Duprex WP.** 2014. Pathological consequences of systemic measles virus infection. J Pathol **235:**253–265. http://dx.doi.org/10.1002/path.4457.
17. **Rima BK, Duprex WP.** 2006. Morbilliviruses and human disease. J Pathol **208:**199–214. http://dx.doi.org/10.1002/path.1873.
18. **Vandevelde M, Zurbriggen A.** 2005. Demyelination in canine distemper virus infection: a review. Acta Neuropathol **109:**56–68. http://dx.doi.org/10.1007/s00401-004-0958-4.
19. **Muller CF, Fatzer RS, Beck K, Vandevelde M, Zurbriggen A.** 1995. Studies on canine distemper virus persistence in the central nervous system. Acta Neuropathol **89:**438–445. http://dx.doi.org/10.1007/BF00307649.
20. **Beineke A, Puff C, Seehusen F, Baumgartner W.** 2009. Pathogenesis and immunopathology of systemic and nervous canine distemper. Vet Immunol Immunopathol **127:**1–18. http://dx.doi.org/10.1016/j.vetimm.2008.09.023.
21. **Ehrengruber MU, Ehler E, Billeter MA, Naim HY.** 2002. Measles virus spreads in rat hippocampal neurons by cell-to-cell contact and in a polarized fashion. J Virol **76:**5720–5728. http://dx.doi.org/10.1128/JVI.76.11.5720-5728.2002.
22. **Lawrence DM, Patterson CE, Gales TL, D'Orazio JL, Vaughn MM, Rall GF.** 2000. Measles virus spread between neurons requires cell contact but not CD46 expression, syncytium formation, or extracellular virus production. J Virol **74:**1908–1918. http://dx.doi.org/10.1128/JVI.74.4.1908-1918.2000.
23. **Makhortova NR, Askovich P, Patterson CE, Gechman LA, Gerard NP, Rall GF.** 2007. Neurokinin-1 enables measles virus trans-synaptic spread in neurons. Virology **362:**235–244. http://dx.doi.org/10.1016/j.virol.2007.02.033.
24. **Duprex WP, McQuaid S, Roscic-Mrkic B, Cattaneo R, McCallister C, Rima BK.** 2000. In vitro and in vivo infection of neural cells by a recombinant measles virus expressing enhanced green fluorescent protein. J Virol **74:**7972–7979. http://dx.doi.org/10.1128/JVI.74.17.7972-7979.2000.
25. **Wyss-Fluehmann G, Zurbriggen A, Vandevelde M, Plattet P.** 2010. Canine distemper virus persistence in demyelinating encephalitis by swift intracellular cell-to-cell spread in astrocytes is controlled by the viral attachment protein. Acta Neuropathol **119:**617–630. http://dx.doi.org/10.1007/s00401-010-0644-7.
26. **Zurbriggen A, Graber HU, Wagner A, Vandevelde M.** 1995. Canine distemper virus persistence in the nervous system is associated with noncytolytic selective virus spread. J Virol **69:**1678–1686.
27. **Watanabe S, Shirogane Y, Suzuki SO, Ikegame S, Koga R, Yanagi Y.** 2013. Mutant fusion proteins with enhanced fusion activity promote measles virus spread in human neuronal cells and brains of suckling hamsters. J Virol **87:**2648–2659. http://dx.doi.org/10.1128/JVI.02632-12.
28. **Avila M, Alves L, Khosravi M, Ader-Ebert N, Origgi F, Schneider-Schaulies J, Zurbriggen A, Plemper RK, Plattet P.** 2014. Molecular determinants defining the triggering range of prefusion F complexes of canine distemper virus. J Virol **88:**2951–2966. http://dx.doi.org/10.1128/JVI.03123-13.
29. **de Vries RD, Mesman AW, Geijtenbeek TB, Duprex WP, de Swart RL.** 2012. The pathogenesis of measles. Curr Opin Virol **2:**248–255. http://dx.doi.org/10.1016/j.coviro.2012.03.005.
30. **Sato H, Yoneda M, Honda T, Kai C.** 2012. Morbillivirus receptors and tropism: multiple pathways for infection. Front Microbiol **3:**75. http://dx.doi.org/10.3389/fmicb.2012.00075.
31. **Leonard VH, Sinn PL, Hodge G, Miest T, Devaux P, Oezguen N, Braun W, McCray PB, Jr, McChesney MB, Cattaneo R.** 2008. Measles virus blind to its epithelial cell receptor remains virulent in rhesus monkeys but cannot cross the airway epithelium and is not shed. J Clin Invest **118:**2448–2458.
32. **Sawatsky B, Wong XX, Hinkelmann S, Cattaneo R, von Messling V.** 2012. Canine distemper virus epithelial cell infection is required for clinical disease but not for immunosuppression. J Virol **86:**3658–3666. http://dx.doi.org/10.1128/JVI.06414-11.
33. **Plattet P, Zweifel C, Wiederkehr C, Belloy L, Cherpillod P, Zurbriggen A, Wittek R.** 2004. Recovery of a persistent canine distemper virus expressing the enhanced green fluorescent protein from cloned cDNA. Virus Res **101:**147–153. http://dx.doi.org/10.1016/j.virusres.2004.01.002.
34. **Langedijk JP, Janda J, Origgi FC, Orvell C, Vandevelde M, Zurbriggen A, Plattet P.** 2011. Canine distemper virus infects canine keratinocytes and immune cells by using overlapping and distinct regions located on one side of the attachment protein. J Virol **85:**11242–11254. http://dx.doi.org/10.1128/JVI.05340-11.
35. **Rivals JP, Plattet P, Currat-Zweifel C, Zurbriggen A, Wittek R.** 2007. Adaptation of canine distemper virus to canine footpad keratinocytes modifies polymerase activity and fusogenicity through amino acid substitutions in the P/V/C and H proteins. Virology **359:**6–18. http://dx.doi.org/10.1016/j.virol.2006.07.054.
36. **Plattet P, Rivals JP, Zuber B, Brunner JM, Zurbriggen A, Wittek R.** 2005. The fusion protein of wild-type canine distemper virus is a major determinant of persistent infection. Virology **337:**312–326. http://dx.doi.org/10.1016/j.virol.2005.04.012.
37. **Zipperle L, Langedijk JP, Orvell C, Vandevelde M, Zurbriggen A, Plattet P.** 2010. Identification of key residues in virulent canine distemper virus hemagglutinin that control CD150/SLAM-binding activity. J Virol **84:**9618–9624. http://dx.doi.org/10.1128/JVI.01077-10.
38. **Plattet P, Langedijk JP, Zipperle L, Vandevelde M, Orvell C, Zurbriggen A.** 2009. Conserved leucine residue in the head region of morbillivirus fusion protein regulates the large conformational change during fusion activity. Biochemistry **48:**9112–9121. http://dx.doi.org/10.1021/bi9008566.
39. **Villarreal LP, Witzany G.** 2013. Rethinking quasispecies theory: from fittest type to cooperative consortia. World J Biol Chem **4:**79–90. http://dx.doi.org/10.4331/wjbc.v4.i4.79.
40. **Duprex WP, McQuaid S, Hangartner L, Billeter MA, Rima BK.** 1999. Observation of measles virus cell-to-cell spread in astrocytoma cells by using a

green fluorescent protein-expressing recombinant virus. J Virol **73:**9568–9575.

41. **Singethan K, Hiltensperger G, Kendl S, Wohlfahrt J, Plattet P, Holzgrabe U, Schneider-Schaulies J.** 2010. *N*-(3-Cyanophenyl)-2-phenylacetamide, an effective inhibitor of morbillivirus-induced membrane fusion with low cytotoxicity. J Gen Virol **91:**2762–2772. http://dx.doi.org/10.1099/vir.0.025650-0.
42. **Wenzlow N, Plattet P, Wittek R, Zurbriggen A, Grone A.** 2007. Immunohistochemical demonstration of the putative canine distemper virus receptor CD150 in dogs with and without distemper. Vet Pathol **44:**943–948. http://dx.doi.org/10.1354/vp.44-6-943.
43. **Rima BK, Duprex WP.** 2005. Molecular mechanisms of measles virus persistence. Virus Res **111:**132–147. http://dx.doi.org/10.1016/j.virusres.2005.04.005.
44. **Meertens N, Stoffel MH, Cherpillod P, Wittek R, Vandevelde M, Zurbriggen A.** 2003. Mechanism of reduction of virus release and cell-cell fusion in persistent canine distemper virus infection. Acta Neuropathol **106:**303–310. http://dx.doi.org/10.1007/s00401-003-0731-0.
45. **Ader N, Brindley M, Avila M, Orvell C, Horvat B, Hiltensperger G, Schneider-Schaulies J, Vandevelde M, Zurbriggen A, Plemper RK, Plattet P.** 2013. Mechanism for active membrane fusion triggering by morbillivirus attachment protein. J Virol **87:**314–326. http://dx.doi.org/10.1128/JVI.01826-12.
46. **Delpeut S, Noyce RS, Richardson CD.** 2014. The tumor-associated marker, PVRL4 (nectin-4), is the epithelial receptor for morbilliviruses. Viruses **6:**2268–2286. http://dx.doi.org/10.3390/v6062268.
47. **Summers BA, Greisen HA, Appel MJ.** 1979. Early events in canine distemper demyelinating encephalomyelitis. Acta Neuropathol **46:**1–10. http://dx.doi.org/10.1007/BF00684797.